INTERNATIONAL JOURNAL OF REMOTE SENSING, 2017
VOL. 39, NO. 5, 1–22
https://doi.org/10.1080/01431161.2017.1404163

ARTICLE

Cross-validation of two liquid water path retrieval algorithms applied to ground-based microwave radiation measurements by the RPG-HATPRO instrument

Vladimir S. Kostsov, Dmitry V. Ionov, Egor Yu. Biryukov and Nikita A. Zaitsev

Department of Atmospheric Physics, Faculty of Physics, St. Petersburg State University, St.Petersburg, Russia

ABSTRACT

A built-in operational regression algorithm (REA) of liquid water path (LWP) retrieval supplied by the manufacturer of the RPG-HATPRO microwave (MW) radiometer has been compared to a so-called physical algorithm (PHA) based on the inversion of the radiative transfer equation. The comparison has been performed for different scenarios of MW observations by the RPG-HATPRO instrument that has been operating at St. Petersburg University since June 2012. The data for the scenarios have been collected within the time period December 2012–December 2014. The estimations of bias and random error for both REA and PHA have been obtained. Special attention has been paid to the analysis of the quality of the LWP retrievals before and after rain events that have been detected by the built-in rain sensor. The estimation has been done of the time period after a rain event when the retrieval quality should be considered as insufficient.

ARTICLE HISTORY
Received 14 April 2017
Accepted 6 November 2017

1. Introduction

Remote-sensing techniques for monitoring the liquid water path (LWP) are not numerous. A technique based on atmospheric microwave (MW) radiation measurements is one of the most advantageous due to its possibility to operate under nearly all weather conditions, continuously, automatically, and with high temporal resolution. This technique is widely used for ground-based observations and space-borne observations over oceans. Physical fundamentals of the ground-based MW radiometry including the basis for LWP derivation and also the examples of modern instruments are presented in the article by Westwater et al. (2005).

Since June 2012, the RPG-HATPRO MW profiler is routinely operating with sampling interval of 1–2 s at the measurement site of the Department of Atmospheric Physics, Faculty of Physics, St. Petersburg State University. The data products – temperature profile, humidity profile, integrated water vapour (IWV), and LWP – are obtained by two independent and separate algorithms: the built-in operational regression algorithm (REA) supplied by the manufacturer of the instrument and the so-called physical

CONTACT Vladimir S. Kostsov vlad@troll.phys.spbu.ru Department of Atmospheric Physics, Faculty of Physics, St. Petersburg State University, 198504 St. Petersburg-Petrodvorets, Ulyanovskaya 1, Russia

algorithm (PHA) based on the inversion of the radiative transfer equation which has been developed at St. Petersburg University and tuned specially for a RPG-HATPRO instrument. The present article deals with LWP retrieval only and considers several problems which still arise in the process of LWP derivation from ground-based MW measurements.

- The problem of the validation of obtained LWP values.
- The problem of error assessment including bias estimation.
- The problem of the retrieval quality assessment and spurious data rejection.

The ways to validate the LWP retrieval results obtained from MW measurements and to estimate the accuracy are not numerous. One of them is to consider the clear-sky conditions when the LWP values should be zero. This approach has been used by Turner et al. (2007) who analysed the accuracy of LWP retrieval from the 2-channel radiometer data (23.8 and 31.4 GHz). Turner et al. (2007) also developed a combination of statistical and physical retrieval algorithms aimed to improve the quality of LWP data obtained from 2-channel MW radiometer measurements. The problems of bias estimation and spurious data rejection during and after rain events were considered in the article by Meijgaard and Crewell (2005): it has been indicated that the problem of rain detection is crucial for data analysis since observations are non-meaningful as long as the water on the instrument has not completely evaporated. It has been reported that generally, within 1 h time period after a rain event, data should be filtered out. In order to assess MW radiometer inferred LWP biases originating from instrumental drifts and uncertainties in the retrieval assumptions, Meijgaard and Crewell (2005) used isolation of cloud-free periods and special procedure to quantify bias correction. Rose et al. (2005) also discussed the problem of the contamination of the MW radiometer measurements by precipitation either due to wetting or the precipitation signal itself. It has been stressed that it is of prime importance to detect precisely the moments of time when precipitation starts and when all water is evaporated from radome surface. Rose et al. (2005) have noted that it is nearly impossible to determine the end of the drying period for an individual radiometer without the use of simultaneous measurements by other instruments. Crewell and Löhnert (2003) have stressed that assessment of the accuracy of LWP retrievals is hard to perform because of a lack of sufficient and independent measurements and therefore, a thorough evaluation of the LWP accuracy must be performed theoretically, taking all sources of error into account. Crewell and Löhnert (2003) presented a thorough study of LWP retrieval accuracy and considered several ways of improving it. Extensive study of the nature of LWP retrieval errors relevant to a 2-channel TROWARA radiometer has been done by Mätzler and Morland (2009), and the bias has been attributed to the variable water vapour influence on absorption at 31 GHz. Much attention has been paid by Mätzler and Morland (2009) to the problem of identification and analysis of cloud-free periods.

The main idea of the present article is to answer the question: Is it possible to work out reliable criteria of the quality of LWP retrievals for a stand-alone 14-channel MW radiometer on the basis of the comparison of the LWP values obtained by two different and independent retrieval algorithms?

2. Experimental setup and retrieval algorithms

The 14-channel MW radiometer RPG-HATPRO (generation 3) has been routinely functioning at the measurement site of the Department of Atmospheric Physics of St. Petersburg University (59.88° N, 29.83° E) since June 2012 with sampling interval about 1–2 s and the integration time 1 s. The complete description of radiometers of the RPG-HATPRO type is presented at the website of the manufacturer (http://www.radiometer-physics.de). All information on experimental setup and the measurement site can be found in the article by Kostsov et al. (2016). The following important items relevant to the present study should be stressed.

- Only zenith observations were considered.
- Only the built-in rain sensor was used for rain detection.
- Together with brightness temperature values in all 14 spectral channels and rain sensor data, the data delivered by built-in temperature, humidity, and pressure sensors were also collected and used.

Processing of measurements has been done by two separate and independent retrieval algorithms. The first algorithm is the built-in REA that had been developed by the manufacturer and had been tuned by the manufacturer for St. Petersburg University measurement site on the basis of MW radiative transfer modelling using huge amount of radiosounding data obtained at the radiosounding station which is the nearest to the measurement site. This algorithm has been used without any modifications – all software had been provided by the manufacturer.

The core of REA is the quadratic regression relationship between the input data and unknown parameters which is given in the 'Instrument Operation and Software Guide',

$$X_i = F_i + \sum_j a_{ij} S_j + \sum_j b_{ij} S_j^2 + \sum_k c_{ik} T_k + \sum_k d_{ik} T_k^2 \qquad (1)$$

where X_i is the ith unknown parameter, F_i is the offset term, S_j is the reading of the jth surface sensor, T_k is the brightness temperature in the kth spectral channel; *a, b, c, d* are the regression coefficients. It should be noted that $j = 1$ when the LWP is retrieved (only pressure surface sensor reading is used). The regression coefficients are derived on the basis of multiple radiative transfer calculations – simulations of radiometric measurements under a variety of atmospheric conditions. The vertical profiles of atmospheric parameters for these simulations are taken from radiosoundings (pressure, temperature, humidity) and from modelling (cloud parameters).

The second algorithm is based on the inversion of the radiative transfer equation and therefore is referred below as PHA. This algorithm uses the well known and widely applied approach of simultaneous retrieval of profiles of several atmospheric parameters that influence the radiative transfer at frequencies that correspond to spectral channels of a radiometer.

The description of the PHA, estimation of the retrieval accuracy for different parameters, and the examples of retrievals can be found in the article by Kostsov (2015a). Here, we briefly describe only the principal features of the algorithm.

The radiative transfer equation is considered in the linearized form,

$$T_b(\nu_i) - T_{b0}(\nu_i) = \int_0^{s_0} \left[K_p(\nu_i, s)(p(s) - p_0(s))ds\right] + \int_0^{s_0} \left[K_T(\nu_i, s)(T(s) - T_0(s))ds\right] + \int_0^{s_0} \left[K_q(\nu_i, s)(q(s) - q_0(s))ds\right] + \int_0^{s_0} \left[K_w(\nu_i, s)(w(s) - w_0(s))ds\right] \quad (2)$$

where T_b is the brightness temperature of the MW radiation, ν_i is the frequency of the *i*th spectral channel of the radiometer, the subscript '0' denotes the reference atmospheric state used for the linearization, *p* is pressure, *T* is temperature, *q* is absolute humidity, *w* is the cloud liquid water concentration, *s* is the coordinate along the optical path (the altitude in our case) from 0 to s_0, and K_p, K_T, K_q, K_w are the so-called weighting functions. The inverse problem is solved in the vector-matrix form with respect to the combined vector of unknowns,

$$\mathbf{x}^T = (p_1, p_2, \ldots p_L, T_1, T_2, \ldots T_L, q_1, q_2, \ldots q_L, w_1, w_2, \ldots w_L) \quad (3)$$

where indices '1, 2, … *L*' denote spatial coordinates (altitude levels), 'T' denotes transposition. Since the problem is ill-posed, the additional information is necessary for obtaining its solution. We applied the additional information using the general approach described by Kostsov (2015b). Under the general approach, different types of this information are treated as virtual measurements. The system of vector-matrix equations to be solved under the general approach was the following,

$$\begin{cases} \mathbf{y}_1 - \mathbf{y}_{1r} = K_1(\mathbf{x} - \mathbf{x}_r) \\ \ldots\ldots\ldots\ldots \\ \mathbf{y}_i - \mathbf{y}_{ir} = K_i(\mathbf{x} - \mathbf{x}_r) \\ \ldots\ldots\ldots\ldots \\ \mathbf{y}_N - \mathbf{y}_{Nr} = K_N(\mathbf{x} - \mathbf{x}_r) \end{cases} \quad (4)$$

where ***x*** is the vector of unknowns, ***y*** is the vector of actual or virtual measurement, *N* is the total number of actual and virtual measurements ($i = 1, \ldots, N$), the index 'r' denotes the reference values of ***x*** and ***y*** used for linearization of equations describing measurements of different kind, **K** is the linear operator matrix obtained as a result of a linearization. A comprehensive description of all aspects of the general approach can be found in the article by Kostsov (2015b) including the solution of the system (4), error assessment, and examples of presenting *a-priori* and additional information as virtual measurements. The application of the general approach to the described above problem of the inversion of MW radiative transfer equation for the case of RPG-HATPRO measurements is presented and analysed in detail by Kostsov (2015a). Characteristics of measurements (the actual and the virtual ones) that were used in the current version of the PHA are given in Table 1.

The output of PHA consists of many parameters; however, in the present study, only the following ones were used.

- The retrieved LWP value calculated by the integration of retrieved cloud liquid water concentration profile *w*(*s*).
- The estimation of random error of the retrieved LWP value obtained from the error matrix of cloud liquid water concentration profile.
- Retrieval quality flag based on the convergence of solution of the iterative process (0 – successful convergence, 1 – no convergence after 12 iterations, 2 – iteration process failed due to obtained nonrealistic values).

Table 1. Characteristics of the actual and the virtual measurements that were used in the current version of the physical algorithm.

No	Type	Measured value	RMSE
Actual measurements			
1	Microwave by RPG-HATPRO	Brightness temperature	0.1 or 0.2°K depending on spectral channel
2	RPG-HATPRO built-in sensors	*In situ*: Temperature Pressure Relative humidity	 1.0°K 1 mbar 5%
Virtual measurements			
3	*A priori* information on profiles	Temperature profile[a] Relative humidity profile[a] Cloud liquid water concentration profile (was taken equal to 0.001 kg m^{-2} in the altitude range 0.3–5.5 km)	Defined by covariance matrix[a] Defined by covariance matrix[a] Defined by model profile of the cloud liquid water concentration variability
4	Hydrostatic equilibrium constraint	Pressure profile	0.02% deviation from the values corresponding to hydrostatic equilibrium

[a]Covariance matrices and mean profiles have been obtained on the basis of radiosoundings at Voeikovo station (WMO ID 26063) in 2013–2014.

- The value of spectral discrepancy (the mean and the root mean square [RMS] difference between the measured brightness temperature values and the values of T_b calculated using the retrieved profiles of atmospheric parameters).

Before comparing the results obtained by the described algorithms, it is useful to point out the distinctions of the algorithms considering input quantities, methodology, *a priori* information, and the application conditions. Below, we briefly summarize the most important common features and distinctions of the algorithms.

- Both algorithms use brightness temperatures of the downwelling MW radiation in all 14 spectral channels as the main input parameters. Additionally, REA uses the pressure value obtained by the surface sensor. PHA uses the information from all surface sensors – pressure, temperature, and relative humidity.
- REA is based on the quadratic relationship between the LWP and input parameters (except the pressure value obtained by surface sensor) while PHA is based on linearized radiative transfer equation and the nonlinearity is corrected by iterations.
- The output parameter of REA is the LWP value while PHA output is the cloud liquid water vertical profile that is further integrated to produce the LWP value. Besides, PHA provides temperature, pressure, and humidity vertical profiles as the output.
- Both methods utilize the radiosounding data as *a priori* information; however, the time periods when these data were obtained are different for PHA and REA. The other distinction is the form of utilization of this information: the input for multiple radiative transfer calculations for REA, and the mean profiles and covariance matrices for PHA.
- As far as the application conditions are concerned, there are no restrictions; both methods are expected to work well for St. Petersburg region during all seasons since the *a priori* information was collected from local radiosounding station.

To our opinion, the most important distinctions of the algorithms are (1) the pre-defined quadratic relationship between the input and output parameters for REA while the nonlinearity is corrected by iterations in PHA; (2) the multi-parameter formulation of the inverse problem for PHA in contrast to single-parameter inverse problem for REA.

3. Measurement data and scenarios for analysis

In the article of Kostsov et al. (2016), the MW observations at the measurement site of St. Petersburg University have been analysed by means of the information approach that included calculations of the information volume and other characteristics of information content for various data ensembles. These data ensembles had been compiled on the basis of measurements performed within the time period from 1 December 2012 to 30 November 2014. In the present study, we used the data obtained during the same period of time due to the following reasons: (1) the instrument was functioning without failures, (2) the obtained data volume is sufficient for derivation of statistical characteristics. The sampling interval of MW measurements was 1–2 s; however, we used for analysis only the data sampled every 120 s in order to keep the computing time for PHA reasonable on one hand and to keep sufficient amount of data for obtaining statistical characteristics on another hand. The complete data set has been divided into several ensembles corresponding to different scenarios of observations. The description of these ensembles is given in Table 2. The major division has been done on the basis of atmospheric temperature and humidity criterion: the data have been attributed either to warm and humid (WH) or to cold and dry (CD) period. All rain events plus the time periods of 1 hour before and 4 hours after each rain event have been excluded and considered separately. These values of time periods before and after a rain event have been chosen on the basis of preliminary estimations in order to definitely exclude the influence of rain.

Sorting the data has been done in order to fulfil several consecutive tasks.

(1) Estimation of bias and random error for REA and PHA using cloud-free periods of ensembles WH1 and CD1.
(2) Assessment of the agreement between REA and PHA for different atmospheric conditions.

Table 2. Data ensembles used for analysis.

Ensemble	Time period	Comment	Number of measurements
WH1	1 May–30 November 2013 plus 1 May–30 November 2014	Warm and humid atmosphere, no rain[a,c]	144,135
WH2	1 May–30 November 2013 plus 1 May–30 November 2014	Warm and humid atmosphere, rain[b]	52,803
CD1	1 December 2012–30 April 2013 plus 1 December 2013–30 April 2014	Cold and dry atmosphere, no rain[a]	135,940
CD2	1 December 2012–30 April 2013 plus 1 December 2013–30 April 2014	Cold and dry atmosphere, rain[b]	24,602

[a]Rain events plus 1 hour before and 4 hours after each rain event have been excluded from consideration.
[b]Only rain events plus 1 hour before and 4 hours after each rain event have been considered.
[c]Several days (19 August–4 September 2013) have been excluded from analysis since the anomalous bias of 0.17 kg m^{-2} has been detected in the REA results.

(3) Analysis of the behaviour of LWP obtained by REA and PHA just before and after rain events for different atmospheric conditions using WH2 and CD2 data.

For the WH period, the number of measurements under rain conditions constitutes 26% of the number of measurements under non-rainy conditions. For the CD period, this value is 15%.

4. Assessment of the bias and the retrieval error

For the assessment of the bias, we followed the approach used by Cossu, Hocke, and Mätzler (2015) who fitted the distribution of LWP values in clear-sky conditions with a single-term Gaussian model. The standard deviation gives the instrument random error σ and the mean value gives the bias b.

Identification of cloud-free periods has been done following the approach by Mätzler and Morland (2009): situations without clouds have been detected by very low standard deviation of the retrieved LWP values within a certain period of time. Each of the data ensembles WH1 and CD1 has been considered as a series of consecutive 1-hour time periods. For every period, the LWP mean value and the standard deviation have been calculated. For simplicity, we use designations b and σ for these quantities, since the lowest values of the quantity σ can be attributed to the random retrieval error and the corresponding b values can be attributed to the bias. The procedure has been applied to the results of both retrieval algorithms (PHA and REA). Figure 1 presents 1-hour mean value of LWP b as a function of corresponding 1-hour RMS variation of LWP σ for two algorithms and two data ensembles. For the illustrative purposes, we have also marked the occurrence of cloud-free conditions as detected by the observers during ground-based spectroscopic Fourier-transform infrared (FTIR) measurements of direct solar radiation that have been carried out at St. Petersburg University measurement site [http://www.ndsc.ncep.noaa.gov/sites/stat_reps/stpetersburg/]. These situations are shown using the FTIR flag value which is equal to unity when FTIR measurements are performed. As it can be seen from Figure 1, the majority of FTIR observations actually correspond to the lower values of σ. The results obtained by PHA exhibit explicit dependence $b(\sigma)$ for small values of σ (0.002–0.005 kg m^{-2}) and so, the smallest values of b and σ can be used for derivation of bias and random error. The results obtained by REA show no dependence of b from σ at all and lead to the conclusion that the bias of the REA results is unstable and highly variable. So, it is impossible to estimate it from the REA results only since the cloud-free situations cannot be identified from the REA results.

For the assessment of bias and random error of PHA, 300 data points have been selected from WH1 and CD1 ensembles that correspond to the lowest values of σ (see Figure 2). We consider that 300 × 1 = 300 hours of observations during cloud-free periods are enough for derivation of bias and random error. So, the mean values of b and σ obtained from these 300 data points have been accepted as the estimates of bias and random error for ensembles WH1 and CD1. Figure 2 demonstrates the overlapping of data corresponding to two ensembles; however, the range of σ values corresponding to WH1 ensemble is about 2 times larger than the range of σ corresponding to the CD1 ensemble. The mean of b and σ calculated from 300 values of these quantities has been taken as the estimates of bias and random error of LWP retrieval.

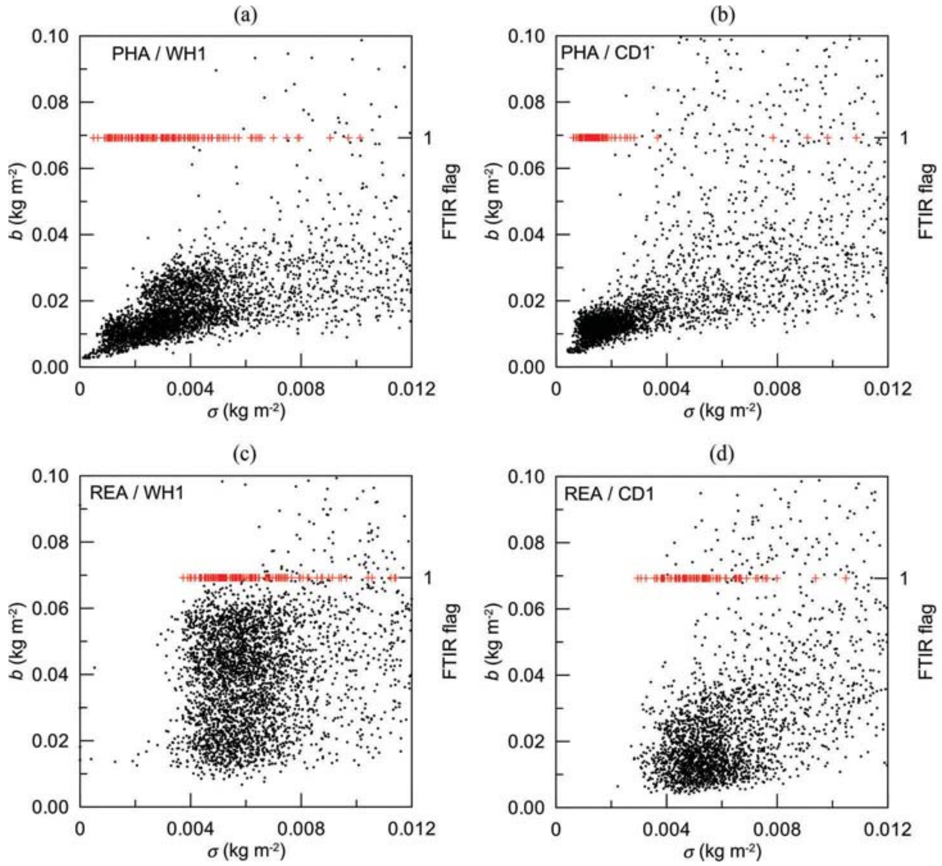

Figure 1. 1-hour mean value of LWP *b* as a function of corresponding 1-hour RMS variation of LWP *σ* for physical algorithm PHA (a, b) and regression algorithm REA (c, d). Data ensembles used WH1 (a, c) and CD1 (b, d). The *b* data greater than 0.10 kg m^{-2} and the *σ* data greater than 0.012 kg m^{-2} are not shown. Red crosses designate the presence of synchronous FTIR measurements (FTIR flag equal to unity), see text for detailed explanation.

After that, we used exactly the same time periods (300 hours total) in order to obtain the bias and random error of REA. The *σ* values of REA appeared to be nearly constant; so, the mean value of *σ* calculated over all 300 hours was taken as the estimate of random error. The *b* and *σ* values of PHA and *σ* values of REA are given in Table 3. The *b* values of REA are time-dependent and not presented in the Table. The difference between the *b* values obtained for PHA for different ensembles can be considered negligible. Therefore, we adopted the value of *b* for PHA equal to 0.010 kg m^{-2} for the whole 2 years period under analysis. For PHA and REA, *σ* is equal to 0.001 and 0.005 kg m^{-2} correspondingly. For the sake of comparison in Table 3, we also presented the values of bias and random error obtained for different ground-based MW instruments and algorithms and reported previously by different authors. We note good agreement between all estimates.

The time dependence of the *b* values for REA is shown in Figure 3(b). The reason for such variability is a very large sensitivity of REA to the presence of spurious values in the input data since the regression scheme is quadratic but not linear. The corresponding

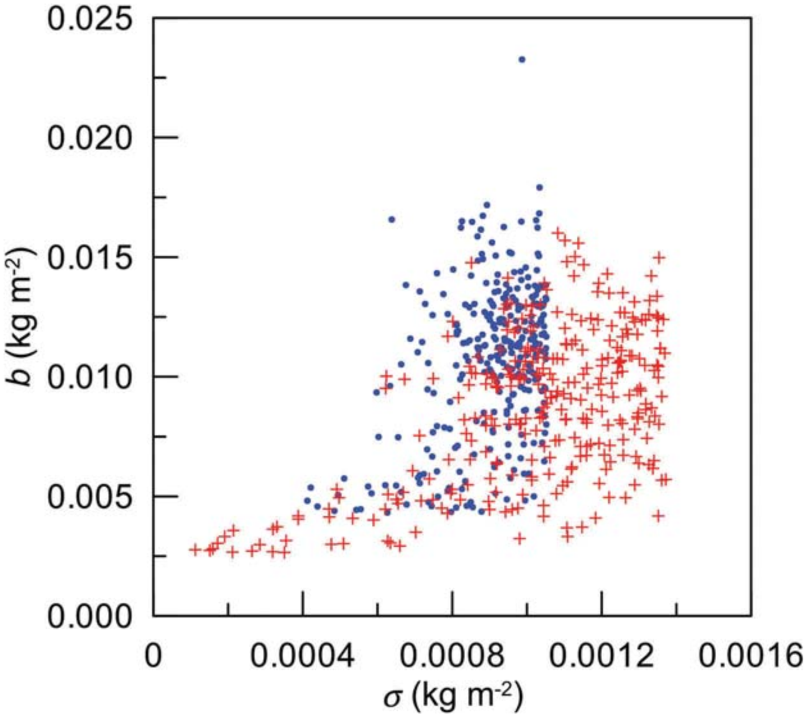

Figure 2. 1-hour mean value of LWP b as a function of corresponding 1-hour RMS variation of LWP σ for physical algorithm PHA and for the lowest 300 values of σ. Data ensembles: WH1 (red crosses) and CD1 (blue dots).

Table 3. The estimations of bias b and random error σ for LWP retrievals taken from different sources.

Reference	b (kg m^{-2})	σ (kg m^{-2}) or (%)
This study, PHA	0.009 for ensemble WH1 0.011 for ensemble CD1	0.001 at low liquid water contents for both ensembles
This study, REA	Highly variable	0.005 at low liquid water contents for both ensembles
Mätzler and Morland (2009)	0.002–0.005	0.001
Cossu, Hocke, and Mätzler (2015)	0.01–0.02	10–20% for LWP > 0.1 kg m^{-2}

results obtained by PHA do not show any peculiarities (Figure 3(a)). When removing the bias from the REA data, we used linear interpolation of the estimates shown in Figure 3(b). For PHA, the constant value 0.010 kg m^{-2} has been used. One can see from Figure 3 that there are two large time intervals in which no cloud-free days have been identified by the 'minimum standard deviation' method. These large intervals are 199–288 and 576–690 days since 1 December 2012, 00 hours 00 minutes. Therefore, the results within these intervals have been analysed specially and it has been found that the results of the REA exhibited extremely high bias of 0.17 kg m^{-2} from 261 days until 277 days. The reason for this anomalous bias was probably multiple instrumental artefacts and all measurements during 261–277 days have been excluded from further analysis.

Concluding this section, we present the random error of LWP retrieval by PHA estimated from the error matrix calculations σ_{em} ('em' stands for 'error matrix'). At the final

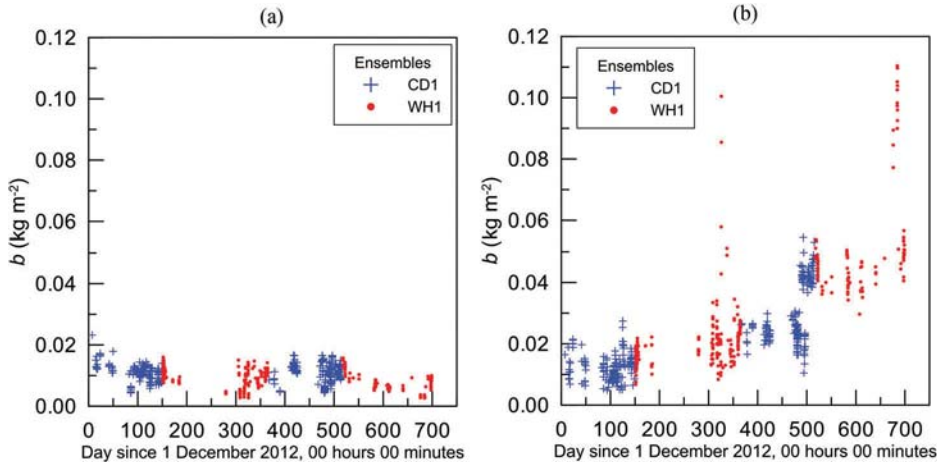

Figure 3. The bias of PHA (a) and REA (b) as a function of time. Every data point corresponds to 1-hour cloud-free period identified from the results of PHA.

iteration step of each retrieval by PHA, the combined error matrix was calculated for the set of unknowns (temperature, pressure, humidity, and liquid water profiles). The σ_{em} was obtained from the block of the combined matrix that corresponded to liquid water profile. It is shown in Figure 4 as a function of LWP value. First, we pay attention to the fact that maximum variability of σ_{em} is observed for the lower values of LWP. The σ_{em} values for the ensemble WH1 and LWP less than 0.1 kg m^{-2} are in the range of 0.002–0.008 kg m^{-2}. The similar situation takes place for the ensemble CD1; however, the range of σ_{em} is noticeably smaller: 0.001–0.005 kg m^{-2}. Second, we note that the mean values of σ_{em} are comparable to the estimations made on the basis of analysis of cloud-free periods that was described above and constitute 0.004 kg m^{-2} for the WH1 ensemble and 0.003 kg m^{-2} for the CD1 ensemble. Third, it is clearly seen that the number of LWP retrievals exceeding 0.4 kg m^{-2} is very small if compared to the results that are lower than this value. This fact is important

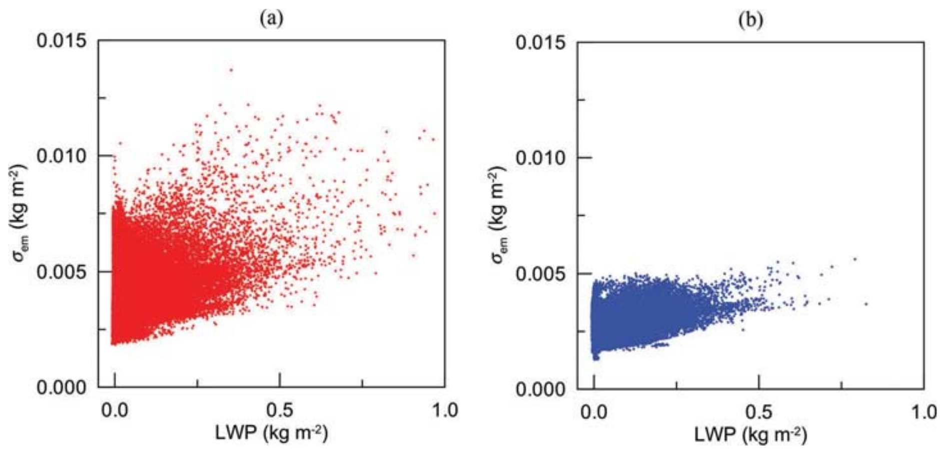

Figure 4. The LWP random error of PHA estimated from the error matrix calculations as a function of retrieved LWP value for the ensemble WH1 (a) and for the ensemble CD1 (b).

since the value 0.4 kg m^{-2} has been reported earlier as a threshold LWP between non-rainy and rainy atmosphere (Mätzler 1992).

5. Analysis of the results obtained under rain-free conditions

One can have the general impression of the agreement between the LWP retrieval results obtained by two algorithms from Figure 5. This scatter plot demonstrates that

- for LWP values greater than about 0.3 kg m^{-2} for the WH1 ensemble and 0.2 kg m^{-2} for the CD1 ensemble, the REA results systematically exceed the PHA results;
- the discrepancy between the results is larger for lower LWP values; and
- there is a certain number of spurious data points with considerable discrepancy between the results.

The presence of spurious data should be analysed separately for every particular case. However, one can propose several reasons leading to considerable mismatch. The first reason is the highly variable bias of REA. Moreover, the variation of this bias can be very rapid in time. The origin of such a behaviour is discussed below. The second possible reason could be the precipitation events (rain or snowfall) that are not detected by the rain sensor. As noted by Löhnert and Crewell (2003), light rain can evaporate on its way to the ground and rain may also be present but may not reach the radiometer due to wind shear. It should be stressed that the analysis has shown the random character of appearance of spurious data, for example during the periods May–June 2013 and December 2013–June 2014, the number of spurious data was negligibly small (1–2 data points).

The agreement between the results obtained by two algorithms for low values of LWP can be demonstrated by comparing the values of cloud fraction (CF). CF is an important quantity which can be derived from MW LWP observations using the approach proposed by Cossu, Hocke, and Mätzler (2015). According to this approach, the clear-sky conditions are filtered out using the criterion,

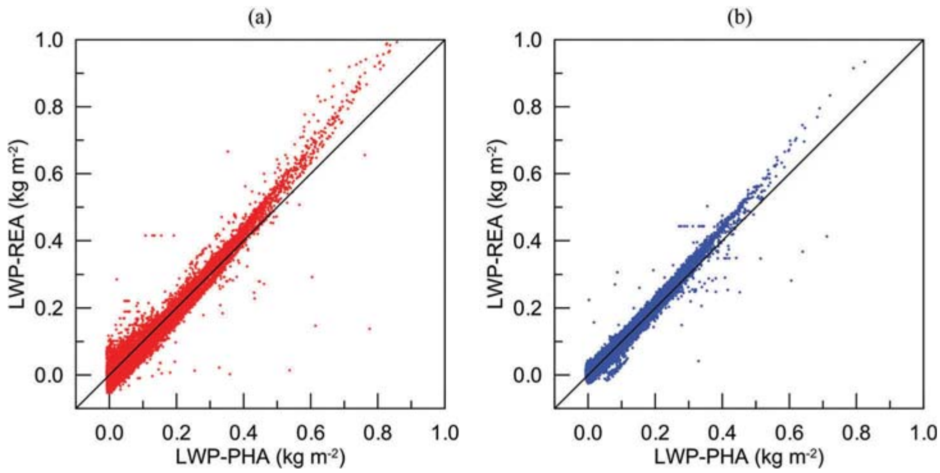

Figure 5. The scatter plot of LWP values obtained by PHA and REA for the ensembles WH1 (a) and CD1 (b).

$$\mathrm{LWP_{clear}} < 3\sigma \tag{5}$$

where σ is the random retrieval error of minimal LWP values and $\mathrm{LWP_{clear}}$ is the measurement value attributed to clear-sky conditions. The CF value will be

$$\mathrm{CF} = \frac{(N_{\mathrm{all}} - N_{\mathrm{clear}})}{N_{\mathrm{all}}} \tag{6}$$

where N_{all} is the total number of measurements and N_{clear} is the number of measurements under cloud-free conditions. Using the σ values for PHA and REA from Table 2, we have obtained the CF values for the WH1 and CD1 ensembles, see Table 4. We have also calculated the CF values for REA using the value of 'measurement noise' of LWP retrievals declared by manufacturer as not exceeding 0.002 kg m^{-2} (the corresponding threshold is 0.006 kg m^{-2}). First of all, we note that for all thresholds and algorithms, the CF values for two data ensembles are very close to each other. Second, the CF values obtained from REA data for threshold 0.015 kg m^{-2} considerably differ from other CF values and constitute 0.43. CF less than 0.5 seems too low for St. Petersburg climate which is characterized by the influence of the Baltic Sea that results in warm, humid, and short summers and long, moderately cold wet winters. The CF values obtained by REA for threshold 0.006 kg m^{-2} agree well with the values obtained by PHA. These values are in the range 0.6–0.7. This result looks reasonable since it is in agreement with the global cloud amount which varies between 0.56 and 0.74 as derived from space-borne measurements with different instruments and reported by Stubenrauch et al. (2013). In the article of Stubenrauch et al. (2013) the definition of cloud amount ('the ratio between the number of samples that contain clouds and the total number of measured samples') fully corresponds to the definition of CF used in the present study.

The comparison of statistical distributions of LWP values is presented in Figure 6 by two histogram plots. One can see that the number of negative LWP values provided by REA is much greater than provided by PHA, especially for WH conditions. At the same time, the number of high positive LWP values provided by REA is greater than provided by PHA. However, within the LWP range 0–0.4 kg m^{-2} which is characteristic for the majority of non-rainy cases, the distributions obtained by two algorithms are very close to each other.

In Figure 7, we present the mean difference and the RMS difference between LWP values obtained by REA and PHA as a function of time ($\Delta_{\mathrm{mean}} = \mathrm{LWP_{REA}} - \mathrm{LWP_{PHA}}$). Averaging was done over 1 month periods of time. As one can see, no seasonal dependence of the differences can be detected. The RMS difference is about 0.010 kg m^{-2} and the mean difference is mainly within the limits from −0.005 to 0.005 kg m^{-2}. The considerable values of the differences are detected for 2 months only – October and November 2014. As it had been mentioned above, this is one of the periods of highly

Table 4. The estimations of cloud fraction (CF) values obtained for different data ensembles and for different LWP threshold values used for detection of cloud-free situations.

Algorithm		PHA	REA	
Threshold (kg m^{-2})		0.003	0.015	0.006
Data ensemble	CD1	0.68	0.43	0.60
	WH1	0.71	0.43	0.65

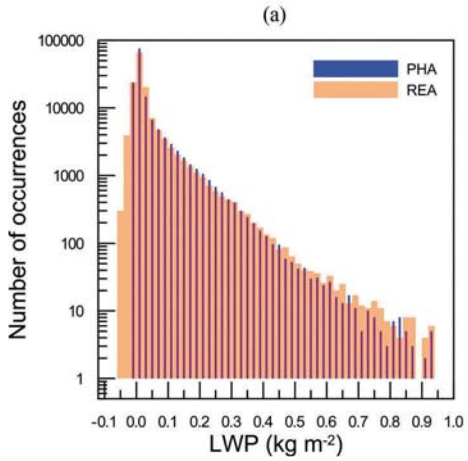

Figure 6. The histogram plot of LWP values obtained by PHA and REA for the ensembles WH1 (a) and CD1 (b).

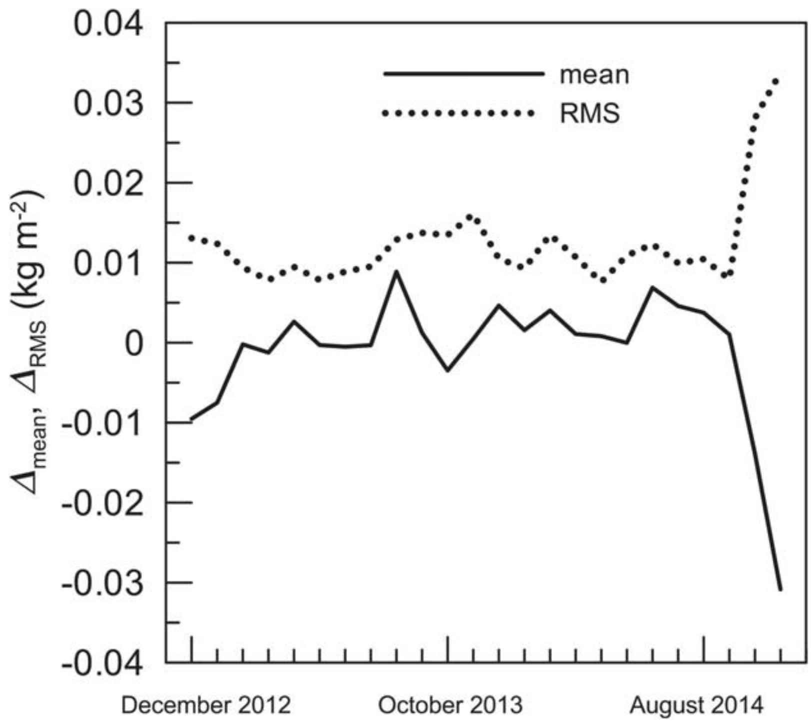

Figure 7. The mean Δ_{mean} and the root mean square Δ_{RMS} difference between LWP values obtained by REA and PHA as a function of time (Δ_{mean} = LWP_{REA} − LWP_{PHA}). Averaging was done over 1 month periods of time.

variable bias of REA (see Figure 3). The consequence of such variability is the presence of multiple errors of bias estimation. In order to illustrate the situation, we present Figure 8 where the results of the LWP retrievals by two algorithms are plotted within the period 15 September 2014–15 October 2014. It is clearly seen that starting from a certain moment of time, the numerous considerably negative values of LWP obtained by REA appeared. The reason is the overestimation of bias for REA.

Concluding this section, we analyse the origin of the considerable sudden changes of the LWP retrieval bias that were detected for the REA. As it has been mentioned above, the period 17 August–4 September 2013 was characterized by the considerable bias of the REA that constituted about 0.17 kg m^{-2}. We selected 4 September 2013 for the analysis since it was a cloud-free day and the moment of the sudden change of bias could be easily identified (at 14:00 UTC). One can see from Figure 9 that the measurements in zenith mode were done with a period of 1–2 s, then there was a break of 106 s and the measurements were resumed again. During this break, the angular scanning mode was in operation. After the angular scanning,

- the REA bias of LWP retrieval became lower by 0.16 kg m^{-2};
- the PHA bias of LWP retrieval became lower by 0.01 kg m^{-2};
- the values of the integrated water vapour obtained by two algorithms increased by 1 kg m^{-2};
- noticeable number of retrievals with the quality flag value of ‘1’ appeared what means that the PHA iteration process did not converge within 12 iterations;
- the brightness temperature values of the channel 22.24 GHz remain unchanged;

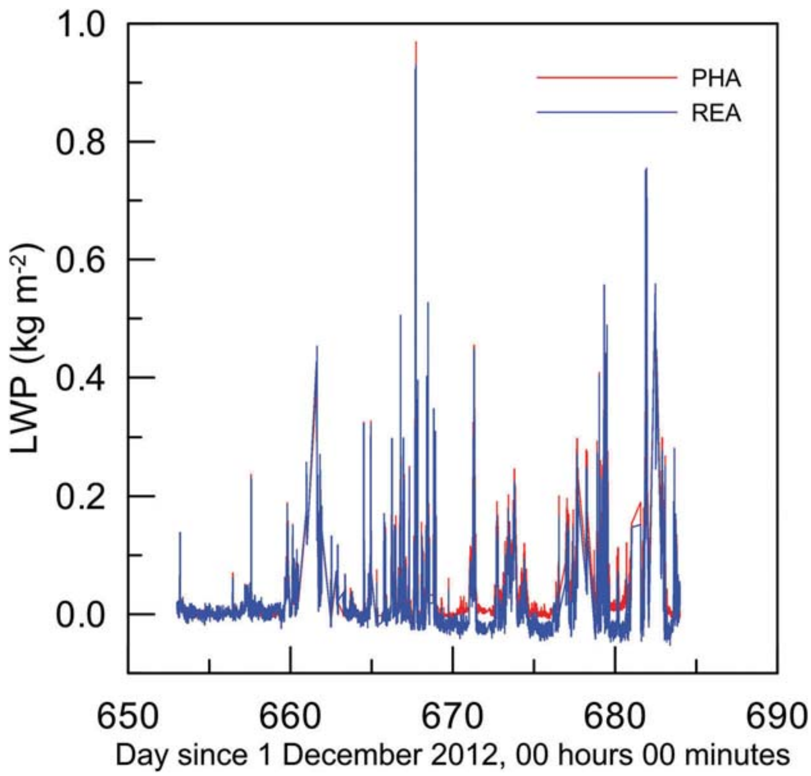

Figure 8. The results of the LWP retrievals by two algorithms within the period 15 September 2014–15 October 2014.

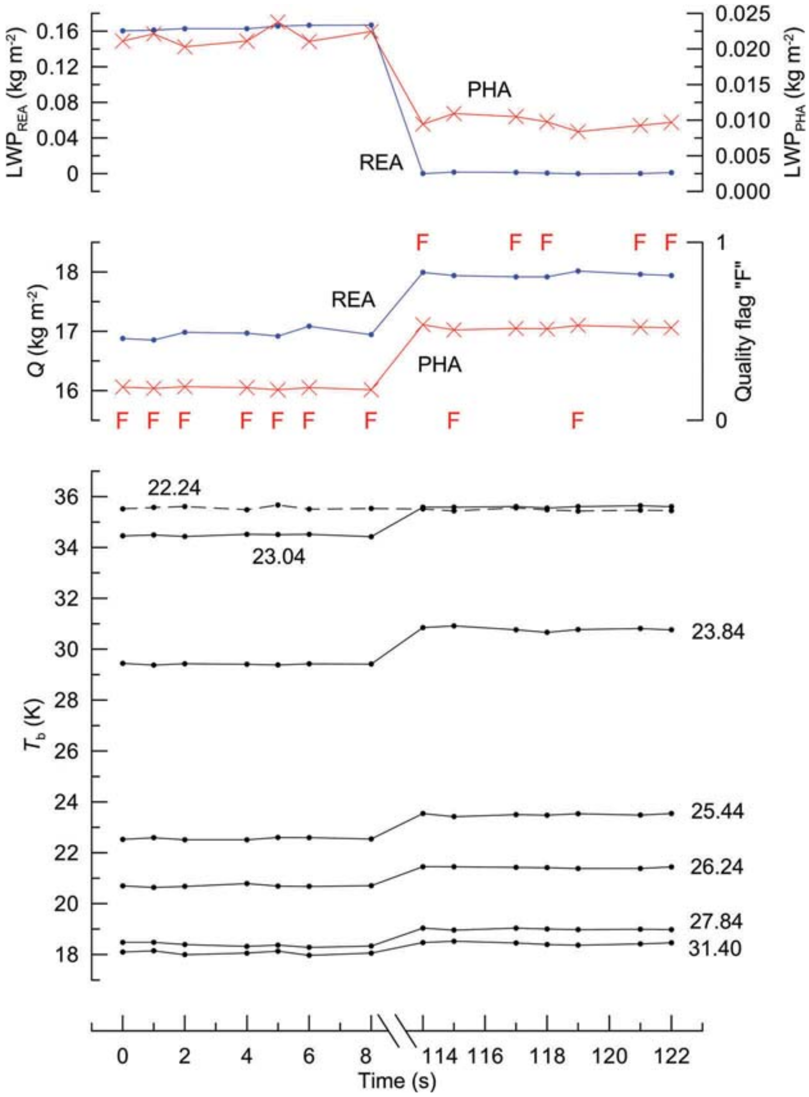

Figure 9. The time chart of the input and output data before and after the moment of sudden change of the LWP retrieval bias (between the 8th and 114th seconds as counted from the moment 4 September 2013 13:59:50 UTC). Top: LWP values retrieved by PHA and REA. Middle: integrated water vapour retrieved by PHA and REA (Q) and the retrieval quality flag 'F' of PHA. Bottom: brightness temperature values in 7 so-called 'humidity channels' (frequencies are given near the curves).

- the brightness temperature values of the channels 23.24–31.4 GHz exhibited the synchronous increase by 0.4–1.4°K; and
- the brightness temperature values of the 'temperature channels' greater than 50 GHz displayed no systematic change (not shown in figure).

We attribute the described change in input data (brightness temperatures) to the instrumental artefact since only channels 2–7 had been affected. The reason for this artefact has not been identified; however, one could guess that it occurred in the process of switching between measurement modes (from zenith mode to angular scanning and back). The most important conclusion is that the quadratic REA for LWP retrieval is very sensitive to such artefacts. The response of REA was 0.17 kg m^{-2} what means about 40% of the maximal LWP value for non-rainy atmosphere if it is taken as 0.4 kg m^{-2}. The response of PHA is 17 times lower and constitutes 0.010 kg m^{-2}. The response of the IWV retrieval by REA and PHA to the instrumental artefact was similar and constituted about 6% of the IWV value.

It should be stressed that such strong instrumental artefact and correspondent REA bias change were unique. The period corresponding to the improbable bias has been excluded from statistical analysis. The origin of REA bias variations observed at other moments of time can be also attributed to instrumental artefacts. Since these variations are considerably lower, we did not remove the correspondent data from ensembles.

6. Analysis of the results obtained just before and after rain events

It has been shown in the previous section that the response of the physical and regression algorithms to the artefact in the input data can be noticeably different. A period during a rain and just after the end of a rain can be considered as a situation that produces artefacts in the input data since the radome of a radiometer is wet and therefore, a radiometer is functioning in an abnormal regime. So, one can expect that the difference between the outputs of REA and PHA will be maximal during a rain and it will become smaller and smaller after a rain event while water evaporates from the surface of the radome. In this section, we investigate whether this fact can be used for the accurate estimation of a radiometer malfunction time after a rain event until all water evaporates from the radome.

The ensembles WH2 and CD2 have been used as a source of LWP data within 4-hour periods after all rain events that occurred from 1 December 2012 to 30 November 2014. These 4-hour periods have been divided into time slots of 10 minutes (the total number of such slots is 24). For every time slot, we have calculated the RMS difference between the LWP values obtained by PHA and REA. The number of data points for each time slot was in the range 1000–3300 which can be considered sufficient for statistical estimations. The results are plotted in Figure 10. As expected, the RMS difference decreases with time passed since the end of a rain. For the CD2 ensemble, the RMS difference becomes comparable with RMS difference for non-rainy conditions (taken as 0.015 kg m^{-2}) after 4 hours since the end of a rain. For the WH2 ensemble, 4 hours is not enough to reach 'non-rainy condition'. After 4 hours, the RMS difference is still considerably high and constitutes about 0.1 kg m^{-2}. In order to estimate the time of reaching non-rainy conditions, we have linearly extrapolated the WH2 data from the 7th time slot to 24th time slot (2–4 hours after a rain event). As it can be seen from Figure 10, the estimated time for the WH2 ensemble is about 22,000 seconds which is roughly 6 hours.

In order to estimate more accurately the duration of the instrument malfunction period after a rain event, it is preferable to use more than one criterion or method. Along with estimation of the RMS difference between the LWP values obtained by PHA and REA, we propose to control the quality flag of the PHA that indicates the convergence of the iteration process. For each 10-minute time slot, we have calculated the so-called quality factor – the ratio of the number of the retrievals with quality flag equal to 1 (no convergence of the iterative process) N_1 to the total number of retrievals N of the PHA,

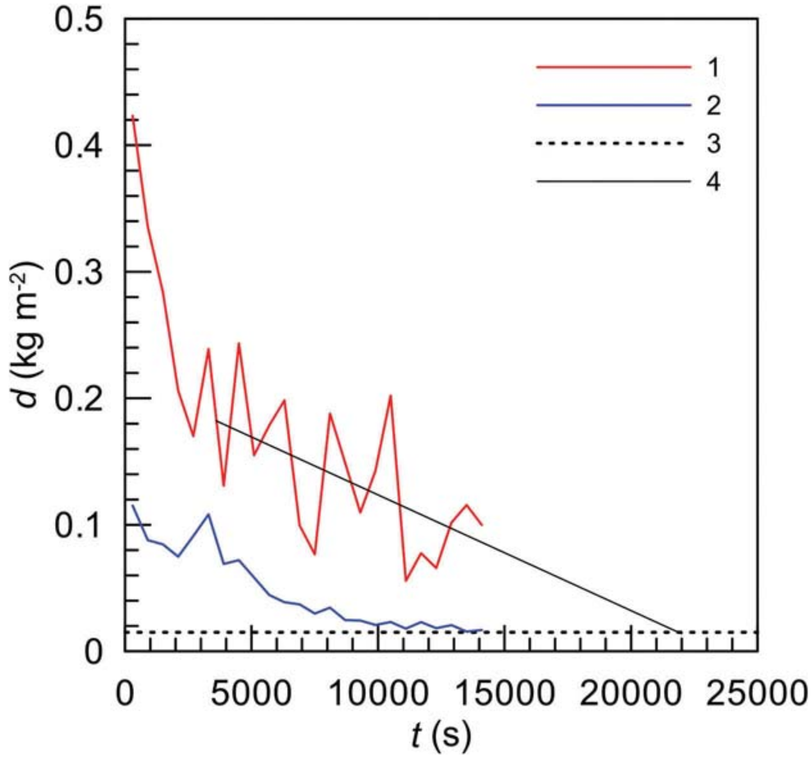

Figure 10. The RMS difference d between the LWP values obtained by PHA and REA as a function of time t passed since the end of a rain: 1 – the WH2 ensemble, 2 – the CD2 ensemble. Line 3 shows the RMS difference for non-rainy conditions. Line 4 is the extrapolation of the data obtained for the WH2 ensemble (see text).

$$f_q = \frac{N_1}{N} \tag{7}$$

The results are presented in Figure 11. One can see that just after end of a rain 50% of retrievals in the WH2 ensemble and 35% of the retrievals in the CD2 ensemble fail (f_q equal to 0.5 and 0.35 correspondingly). After about 2 hours, the number of unconverged retrievals becomes less than 20% for both ensembles and continues to decrease permanently. After 4 hours, the quantity of failed retrievals is still about 10%. In order to estimate the time when unconverged iterations are absent, we linearly extrapolated the data from the 7th time slot to the 24th time slot (2–4 hours after a rain event). This extrapolation indicates that after about 5–5.5 hours, one could expect the complete transfer to the non-rainy conditions.

When removing spurious data after a rain event, two approaches can be used. The first approach is to apply one constant criterion for all rain events that means rejecting all LWP values within the time period of duration t_c after end of a rain. In case of MW measurements with RPG-HATPRO radiometer at St. Petersburg University measurement site, the duration t_c is recommended to be taken equal to 6 hours since this is the largest value among all estimations that have been made and described above. The second

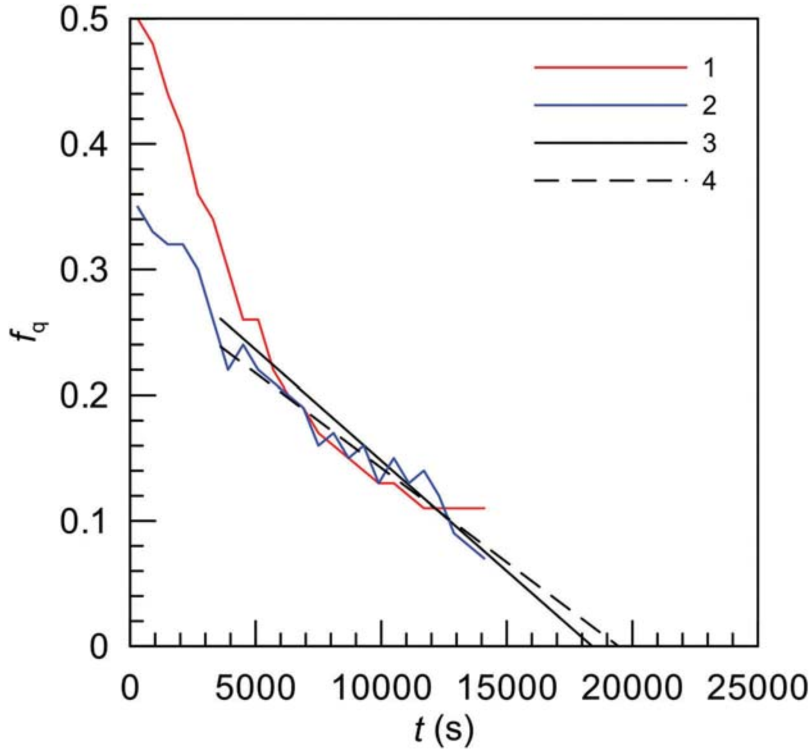

Figure 11. The quality factor of PHA f_q as a function of time t passed since the end of a rain: 1 – for the WH2 ensemble, 2 – for the CD2 ensemble. Lines 3 and 4 present the linear extrapolation of the data obtained for the WH2 and the CD2 ensembles correspondingly (see text).

approach is based on simultaneous control of the difference between the LWP values obtained by PHA and REA and of the quality factor of the PHA for every single rain event. The data are rejected until the quality factor approaches zero and the difference between the LWP values obtained by PHA and REA approaches the value that is characteristic for non-rainy conditions. Below, we present one example of the application of both approaches.

Figure 12 presents the time chart of the parameters used for the assessment of the LWP retrieval quality and rejecting spurious results before and after rain events on 2 August 2013. The 8-hour period of time has been selected on this day. The period starts just after the end of the first rain (the rain sensor flag is stable and equals to zero); this moment of time is designated by t_0. If the general criterion of rejection of all data within 6 hours after a rain is used, all data corresponding to the selected 8-hour period of time should be rejected since 6 hours after t_0, the second rain was already going on. However, the situation is different if we analyse the RMS difference d between the LWP values obtained by PHA and REA simultaneously with the quality factor f_q. Since these quantities are highly variable in time, we used the running average value of d calculated over time slots of 20 minutes and f_q is calculated also for these time slots. At the moment of time t_1, the RMS LWP difference d became lower than the level of d which is characteristic for non-rainy atmosphere. At the same time, the quality factor

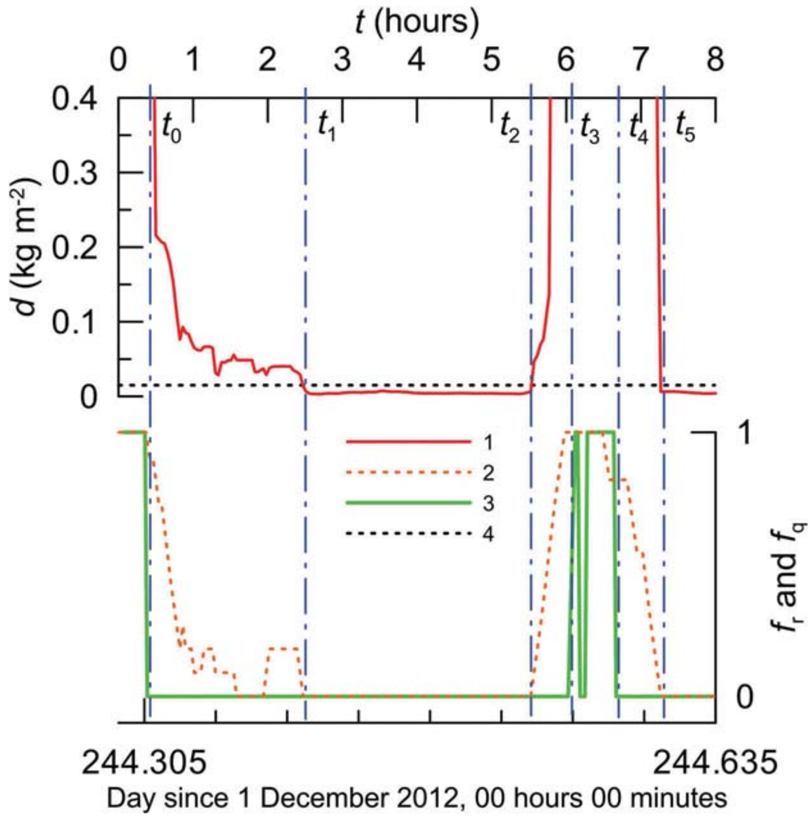

Figure 12. The time chart of the parameters used for the assessment of the retrieval quality before and after rain events on 2 August 2013. 1 – the running average (time slot 20 minutes) of the RMS difference σ of the LWP values obtained by PHA and REA; 2 – the quality factor f_q of the retrievals by PHA (running time slot 20 minutes); 3 – rain sensor flag f_r, 4 – the level of RMS difference of the LWP values obtained by PHA and REA as estimated for non-rainy conditions. Dash-dotted blue lines show specific moments of time t_0–t_5 – see text.

became zero. (Below, we omit the words 'running average' when talking about d and f_q.) All data within the moments $t_1 - t_2$ are valid and can be kept for analysis. It should be stressed that both criteria showed the appearance of spurious data about half an hour earlier ($t = t_2$) than the rain sensor indicated the beginning of the second rain ($t = t_3$). At the moment t_4, the second rain stopped and after about half an hour, both criteria indicated that the data became valid for analysis ($t = t_5$). Concluding this section, we would like to stress the following.

- In case the combination of d- and f_q-criteria is used, there is a good opportunity to increase considerably the amount of non-spurious data for further analysis.
- The critical moments of time (rejection or approval of data) are detected by both criteria synchronically and this fact confirms their applicability for data analysis.
- The criteria work well not only for the periods after rain events but also for the periods just before rain events when the rain sensor does not yet indicate rain but the data should already be rejected.

7. Conclusion

The results of LWP retrievals from the MW radiation measurements made by the RPG-HATPRO radiometer operating at the measurement site of St. Petersburg University have been analysed for the time period December 2012–November 2014. The LWP data were obtained by two different and independent algorithms: PHA, based on the inversion of the radiative transfer equation, and REA, based on multiple radiative transfer modelling. Four data ensembles have been compiled that describe non-rainy and rainy conditions for the WH period of observations and for the CD period as well.

Several problems of LWP derivation from ground-based MW measurements have been considered: (1) the problem of the validation of obtained LWP values; (2) the problem of error assessment including bias estimation; and (3) the problem of the retrieval quality assessment and spurious data rejection. The main goal of the investigations was to work out reliable criteria of the quality of LWP retrievals and to obtain the precise estimations of the retrieval accuracy for a stand-alone 14-channel MW radiometer on the basis of the comparison of the LWP values obtained by two different and independent retrieval algorithms. Special attention has been paid to the analysis of the quality of the LWP retrievals before and after rain events that have been detected by the built-in rain sensor.

The following main results have been obtained.

(1) The identification of cloud-free periods of time using the criterion of minimal observed variations of LWP values can be successfully done using the PHA results. However, this criterion fails for the results obtained by the REA. As a consequence, the PHA data can be considered self-sufficient for the estimation of bias from cloud-free measurements, but for REA data, it is necessary to have independent information on cloud-free periods.

(2) The bias of PHA results is very stable and constitutes 0.010 kg m^{-2}. The random error of the LWP retrieval by PHA has been estimated as 0.001 kg m^{-2} at low liquid water contents. The bias of REA results is highly variable. The reason for the considerable bias change is a very large sensitivity of REA to the presence of spurious values in the input data (the instrumental artefacts) since the regression scheme is quadratic, not linear. The random error of the LWP retrieval by REA has been estimated as 0.005 kg m^{-2} at low liquid water contents.

(3) The random errors of LWP retrieval by PHA for different data ensembles have been derived also from the error matrix calculations at the final iteration step of each retrieval. The obtained mean values are comparable to the estimations made on the basis of analysis of cloud-free periods and constitute 0.004 kg m^{-2} for the WH period and 0.003 kg m^{-2} for the CD period.

(4) The comparison of the PHA and REA results for non-rainy conditions has shown that the RMS difference is about 0.010 kg m^{-2} and the mean difference is mainly within the limits from −0.005 to 0.005 kg m^{-2}. Within the LWP range 0.0–0.4 kg m^{-2}, which is characteristic for the majority of non-rainy cases, the statistical distributions of LWP obtained by two algorithms are very close to each other.

(5) A period during a rain and just after the end of a rain can be considered as a situation that produces artefacts in the input data since the radome of a radiometer is wet and therefore, a radiometer is functioning in an abnormal regime. Since the response of the physical and regression algorithms to an artefact in the

input data can be noticeably different, the discrepancy between the outputs of REA and PHA is maximal during a rain and becomes smaller and smaller after a rain event while water evaporates from the radome. It has been shown that for the CD period, the RMS difference becomes comparable to RMS difference for non-rainy conditions on average after 4 hours since the end of a rain. For the WH period, 4 hours is not enough to reach 'non-rainy condition' on average.

(6) Two approaches for data quality control just before and after a rain have been proposed and tested. The first approach is to apply one constant criterion for all rain events that means rejecting all LWP values within the time period of duration t_c after end of a rain. In case of MW measurements with RPG-HATPRO radiometer at St. Petersburg University measurement site, the duration t_c is recommended to be taken equal to 6 hours. The second approach is based on simultaneous control of the difference between the LWP values obtained by PHA and REA and of the convergence of the iterative process of the PHA for every single rain event. The data are rejected until the number of unconverged retrievals within specific time period becomes zero and the discrepancy between the LWP values obtained by PHA and REA becomes comparable to its value that is characteristic for non-rainy conditions. The second approach works well not only for the periods after rain events but also for the periods just before rain events when the rain sensor does not yet indicate rain but the data should already be rejected.

(7) Since the response of the REA to artefacts in the input data is considerably larger than the response of the PHA and since there are problems with the detection of cloud-free periods from the data obtained by REA, one can come to the conclusion that the utilization of the PHA is more preferable. However, the combination of both gives the additional possibility for data quality control.

Finally, summarizing all results and conclusions, we can answer the main question that has been put in Section 1: yes, it is possible to work out a reliable criteria of the quality of LWP retrievals and to obtain the precise estimations of the retrieval accuracy for a stand-alone 14-channel MW radiometer on the basis of the comparison of the LWP values obtained by two different and independent retrieval algorithms.

Acknowledgement

The operation of the RPG-HATPRO instrument was provided by the Research Center GEOMODEL of St. Petersburg State University (http://geomodel.spbu.ru/).

Disclosure statement

No potential conflict of interest was reported by the authors.

Funding

Measurements and data processing were supported by Russian Science Foundation through the project No. 14-17-00096. Data analysis was supported by Russian Foundation for Basic Research through the project Nos. 16-05-00681 and 15-05-07524.

ORCID

Vladimir S. Kostsov http://orcid.org/0000-0002-6160-6634
Dmitry V. Ionov http://orcid.org/0000-0002-4844-5397
Nikita A. Zaitsev http://orcid.org/0000-0002-6986-3352

References

Cossu, F., K. Hocke, and C. Mätzler. 2015. "A 10-Year Cloud Fraction Climatology of Liquid Water Clouds over Bern Observed by a Ground-Based Microwave Radiometer." *Remote Sensing* 7: 7768–7784. doi:10.3390/rs70607768.

Crewell, S., and U. Löhnert. 2003. "Accuracy of Cloud Liquid Water Path from Ground-Based Microwave Radiometry, 2, Sensor Accuracy and Synergy." *Radio Science* 38 (3): 8042. doi:10.1029/2002RS002634.

Kostsov, V. S. 2015a. "Retrieving Cloudy Atmosphere Parameters from RPG-HATPRO Radiometer Data." *Izvestiya, Atmospheric and Oceanic Physics* 51 (2): 156–166. doi:10.1134/S0001433815020085.

Kostsov, V. S. 2015b. "General Approach to the Formulation and Solution of the Multi-Parameter Inverse Problems of Atmospheric Remote Sensing with Measurements and Constraints of Different Types." *International Journal of Remote Sensing* 36 (11): 2963–2994. doi:10.1080/01431161.2015.1054961.

Kostsov, V. S., Y. M. Timofeyev, N. A. Zaitsev, A. V. Poberovsky, and S. I. Osipov. 2016. "Application of the Information Approach to the Analysis of Two-Year Microwave Observations of the Atmosphere by the RPG-HATPRO Radiometer at St.Petersburg University." *International Journal of Remote Sensing* 37 (14): 3346–3364. doi:10.1080/01431161.2016.1199060.

Löhnert, U., and S. Crewell. 2003. "Accuracy of Cloud Liquid Water Path from Ground-Based Microwave Radiometry 1. Dependency on Cloud Model Statistics." *Radio Science* 38 (3): 8041. doi:10.1029/2002RS002654.

Mätzler, C. 1992. "Ground-Based Observations of Atmospheric Radiation at 5, 10, 21, 35, and 94 GHz." *Radio Science* 27: 403–415. doi:10.1029/91RS03052.

Mätzler, C., and J. Morland. 2009. "Refined Physical Retrieval of Integrated Water Vapor and Cloud Liquid for Microwave Radiometer Data." *Ieee Transactions on Geoscience and Remote Sensing* 47 (6): 1585–1594. doi:10.1109/TGRS.2008.2006984.

Meijgaard, E., and S. Crewell. 2005. "Comparison of Model Predicted Liquid Water Path with Ground-Based Measurements during CLIWA-NET." *Atmospheric Research* 75 (3): 201–226. doi:10.1016/j.atmosres.2004.12.006.

Rose, T., S. Crewell, U. Löhnert, and C. Simmer. 2005. "A Network Suitable Microwave Radiometer for Operational Monitoring of the Cloudy Atmosphere." *Atmospheric Research* 75 (3): 183–200. doi:10.1016/j.atmosres.2004.12.005.

Stubenrauch, C. J., W. B. Rossow, S. Kinne, S. Ackerman, G. Cesana, H. Chepfer, L. D. Girolamo, et al. 2013. "Assessment of Global Cloud Datasets from Satellites: Project and Database Initiated by the GEWEX Radiation Panel." *Bulletin of the American Meteorological Society* 94: 1031–1049. doi:10.1175/BAMS-D-12-00117.1.

Turner, D. D., S. A. Clough, J. C. Liljegren, E. E. Clothiaux, K. E. Cady-Pereira, and K. L. Gaustad. 2007. "Retrieving Liquid Water Path and Precipitable Water Vapor from the Atmospheric Radiation Measurement (ARM) Microwave Radiometers." *IEEE Transactions On Geoscience And Remote Sensing* 45 (11): 3680–3690. doi:10.1109/TGRS.2007.903703.

Westwater, E., S. Crewell, C. Mätzler, and D. Cimini. 2005. "Principles of Surface-Based Microwave and Millimeter Wave Radiometric Remote Sensing of the Troposphere." *Quaderni Della Societa Italiana Di ElettroMagnetismo* 1 (3): 50–90.